Iğdır Üniversitesi Fen Bilimleri Enstitüsü Dergisi, 14(1), 356-362, 2024
Journal of the Institute of Science and Technology, 14(1), 356-362, 2024

ISSN: 2146-0574, eISSN: 2536-4618

Chemistry **DOI: 10.21597/jist.1347906**

Research Article

Received: 22.08.2023 **Accepted: 04.12.2023**

To Cite: Avcı Özbek, H. (2024). Molybdenum–Vanadium Oxide Clusters: Syntheses, Structures and Antibacterial Properties. *Journal of the Institute of Science and Technology*, 14(1), 356-362.

Molybdenum–Vanadium Oxide Clusters: Syntheses, Structures and Antibacterial Properties

Hülya AVCI ÖZBEK[1*]

Highlights:
- Structural characterization
- Metal oxide
- Antimicrobial activity

Keywords:
- Molybdenum
- Molybdovanadate cluster
- Polyoxometalate
- Vanadium

ABSTRACT:

The design and synthesis of polyoxometalates (POMs), a type of inorganic compounds, are of great interest due to their interesting structural properties as well as their extensive theoretical and practical applications in catalysis, electrical conductivity, magnetism, optics and medicine. Therefore, in this study two molybdovanadates $[Cu(phen)_2]_3[Mo_6V_2O_{26}]\cdot 4H_2O$ and $[Cu(bpy)_2]_3[Mo_6V_2O_{26}]\cdot 4H_2O$ have been prepared by the reaction of the $[Mo_6V_2O_{26}]^{6-}$ anion with $Cu(CH_3COO)_2$ and 1,10-phenanthroline/2,2'-bipyridine in aqueous medium; characterized by Fourier Transform Infrared Spectroscopy (FT-IR), Nuclear Magnetic Resonance (1H NMR), Inductively coupled plasma mass spectrometry (ICP-MS), Thermogravimetric Analysis (TGA) and elemental analysis. The compounds show antibacterial activity against Escherichia coli (E. Coli) and Staphylococcus aureus (S. Aureus).

[1] Hülya AVCI ÖZBEK (**Orcid ID:** 0000-0003-1508-2558), Manisa Celal Bayar University, Faculty of Arts and Sciences, Department of Chemistry, Manisa, Türkiye

***Sorumlu Yazar/*Corresponding Author**: Hülya AVCI ÖZBEK[1], e-mail: hulya.avci@cbu.edu.tr

INTRODUCTION

Bacterial diseases are serious threats to human healthcare. Today, millions of people die each year from bacterial diseases. The development of effective antibacterial substances to solve the problem caused by bacterial diseases is attracting more and more attention of scientific researchers (Gong et al., 2023; Hegde et al., 2023; Gong et al., 2023; Yang et al., 2023). Studies on the preparation of new compounds to obtain effective antimicrobial active species are increasing rapidly (Bildirici et al., 2023). POMs in particular are considered to have a promising future in the pharmaceutical industry (Bjelic et al., 2015; Mousavi et al., 2022; Wang et al., 2017).

POMs are a wide family of early transition metal oxide cluster anions with exceptional physical and chemical properties and find application in many areas such as medicine, photoelectric chemistry, magnetism, catalysis and pharmaceuticals (Han et al., 2019; Lentink et al., 2023; Lou et al., 2008; Cetin and Korkmaz, 2018; Cetin et al., 2019; Korkmaz et al., 2023; Song et al., 2022; Xing et al., 2023). Since POMs have synergistic or direct antibacterial activity, some research has focused on the medicinal chemistry of POMs such as antitumour, antiviral and antibacterial have been reported (Avcı Özbek et al., 2021; Bjelic et al., 2015; Zhao et al., 2020).

Although Liebert isolated a molybdovanadate-containing salt with a Mo/V ratio of 6:2 in 1891, it was only with the 1975 elucidation of the Björnberg crystal structure that the $[Mo_6V_2O_{26}]^{6-}$ anion was characterised as isostructural with the $[Mo_8O_{26}]^{4-}$ anion (Björnberg, 1975). In the following years, many new compounds were obtained by investigating the reactions of molibdovanadate anion with different salts and found applications in different fields (Buvailo et al., 2019; Cindrić et al., 2002; Fei et al., 2015; Gao et al., 2019; Wang et al., 2009). Since there are no previous studies in the literature that compounds containing molibdovanadate cluster show antimicrobial activity, this article aims to design novel POMs for biomedical applications and antibacterial activity. Herein, two molybdovanadate cluster modified by $Cu(CH_3COO)_2$ and 1,10-phenanthroline/2,2'-bipyridine namely $[Cu(phen)_2]_3[Mo_6V_2O_{26}]\cdot 4H_2O$ **(1)** and $[Cu(bpy)_2]_3[Mo_6V_2O_{26}]\cdot 4H_2O$ **(2)** which were prepared and studied antibacterial properties.

MATERIALS AND METHODS

General Methods

Chemicals purchased from Sigma-Aldrich were used without purification. $K_5NaMo_6V_2O_{26}\cdot 4H_2O$ was synthesised as described in the literature and characterised by FT-IR (Nenner et al., 1985). FT-IR spectra in the 400-4000 cm^{-1} range were recorded on a Perkin Elmer LR 64912 C spectrometer from a KBr-palletised sample. Elemental analysis was carried out on a LECO-932 CHNS elemental analyser for C, H and N. ICP-MS analyses were carried out using an ICP-MS Agilent Technology 7700. ^{1}H NMR spectra were obtained on an AVANCE III 400 MHz NaNoBay FT-NMR spectrometer operating at 400 MHz (^{1}H) in DMSO-d$_6$. Thermogravimetric analysis (TGA) was performed on a Hitachi Exstar TG/DTA 7300 instrument under nitrogen gas flow between 25 and 800^{o}C at a heating rate of 10^o/min.

Synthesis of New Compounds

$[Cu(phen)_2]_3[Mo_6V_2O_{26}]\cdot 4H_2O$ (1)

$K_5NaMo_6V_2O_{26}\cdot 4H_2O$ was (277 mg, 0.2 mmol) was dissolved in 10 mL H_2O. $Cu(CH_3COO)_2$ (0.102 g, 0.6 mmol) dissolved in 5 mL H_2O (10 mL) and 1,10-phenanthroline (phen) (0.216 g, 1.2 mmol) added to this solution. Afterwards two solutions mixed stirred for 30 min and filtered. The product washed with water and dried at 50 ^{o}C. Yield: 440 mg, 93%. FT-IR data (cm^{-1}): 425 (s), 592 (m), 644 (m), 722 (s), 735 (m), 791 (m), 850 (s), 869 (m), 939 (s), 1308 (m), 1344 (m), 1429 (s), 1457 (m), 1493 (m), 1519 (s), 1585 (m), 1606 (s), 1625 (m), 3056 (m), 3401 (w). Anal. Calcd. (%) for $Cu_3C_{72}H_{56}N_{12}Mo_6V_2O_{30}$ (2310.34 g/mol): C, 35.48; H, 2.32; N, 6.90; Cu, 7.82; Mo, 23.62; V, 4.18. Found (%): C, 34.94; H, 2.17; N, 6.62; Cu, 6.87; Mo, 23.56; V, 3.84. TGA (loss of $4H_2O$): calcd. 2.95%. found 3.1%; (loss of Cu): calcd. 7.82%, found 7.6%; (loss of (1,10-phen)): calcd. 44.35%, found 43.43%. ^{1}H NMR (DMSO-d_6): δ 7.82 (s, 18H, CH), 8.02 (s, 18H, CH), 8.51 (s, 18H, CH), 9.13 (s, 18H, CH).

$[Cu(bpy)_2]_3[Mo_6V_2O_{26}]\cdot 4H_2O$ (2)

The synthesis of **2** was similar to that of **1**, except that 1,10-phenanthroline replaced 2,2'-bipyridine (bpy) (0.18 g, 1.2 mmol). Yield: 265 mg, 56%. FT-IR data (cm^{-1}): 417 (m), 592 (m), 658 (m), 728 (m), 773 (m), 798 (m), 926 (m), 1014 (m), 1031 (m), 1107 (m), 1160 (s), 1173 (s), 1250 (m), 1316 (s), 1442 (s), 1473 (m), 1576 (m), 1598 (m), 3070 (m), 3419 (w). Anal. Calcd. (%) for $Cu_3C_{60}H_{56}N_{12}Mo_6V_2O_{30}$ (2166.22 g/mol): C, 31.42; H, 2.46; N, 7.33; Cu, 8.31; Mo, 25.10; V, 4.44. Found (%): C, 31.03; H, 2.45; N, 6.67; Cu, 7.71; Mo, 25.60; V, 4.00. TGA (loss of $4H_2O$): calcd. 3.14%, found 3.58%; (loss of Cu): calcd. 8.31%, found 8.66%; (loss of (bpy)): calcd. 40.86%, found 41.21%. ^{1}H NMR (DMSO-d_6): δ 7.49 (s, 14H, CH), 7.99 (s, 14H, CH), 8.44 (s, 14H, CH), 8.73 (s, 14H, CH).

Antibacterial analysis

Antibacterial analysis of **1** and **2** was performed by disc diffusion method with gram-positive bacteria *S. aureus* ATCC 25923 and gram-negative bacteria *E. coli* ATCC 25922 according to previous literature (Avcı Özbek, 2023).

RESULTS AND DISCUSSION

Characterization of Compounds

1 and **2** were synthesized by reaction of $K_5NaMo_6V_2O_{26}\cdot 4H_2O$ with $Cu(CH_3COO)_2$ and 1,10-phenanthroline/2,2'-bipyridine in an aqueous medium (Figure 1). Observed elemental (C, H, N) and ICP-MS (Mo, V, Cu) data of **1** and **2** agree well with calculated values. Furthermore, experimentally obtained elemental analyses results and other spectroscopic data (FT-IR, ^{1}H NMR, ICP-MS, and TGA) support **1** and **2** formulated as $[Cu(phen)_2]_3[Mo_6V_2O_{26}]\cdot 4H_2O$ (**1**), $[Cu(bpy)_2]_3[Mo_6V_2O_{26}]\cdot 4H_2O$ (**2**). In this way, the structures of the newly synthesised compounds were found to be similar to those of the compounds already reported (Buvailo et al., 2019; Cindrić et al., 2002; Fei et al., 2015; Gao et al., 2019; Wang et al., 2009).

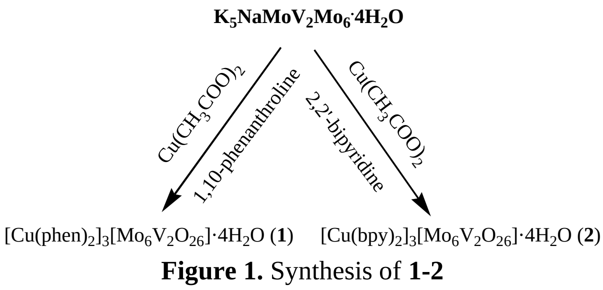

Figure 1. Synthesis of **1-2**

The bands between 1000 and 400 cm^{-1} in the FT-IR spectrum (Figure 2-3) of the octamolybdate cluster can be attributed to the M=O and M-O-M (M = Mo, V) stretching vibrations of POM. The characteristic bands of ν(M=O) (M= Mo, V) vibrations are observed at 939 and 926 cm^{-1} for **1** and **2** respectively; the bands of ν (M–O–M) are at 850, 791, 722 cm^{-1} for **1**, 798, 773, 728 cm^{-1} for **2**. A series of bands for **1**, 1308, 1344, 1429, 1457, 1493, 1519, 1585, 1606 and 1625 cm^{-1} are assigned to the 1,10-phenanthroline groups. A series of bands for **2**, 1014, 1031, 1107, 1160, 1173, 1250, 1316, 1442, 1473, 1576 and 1598 cm^{-1} are assigned to the 2,2'-bipyridine groups. The broad bands at 3200-3450 cm^{-1} are due to ν(O-H) vibrations. This suggests extensive hydrogen bonding interactions. FT-IR results are in agreement with those from previous studies (Buvailo et al., 2019; Cindrić et al., 2002; Fei et al., 2015; Gao et al., 2019; Wang et al., 2009).

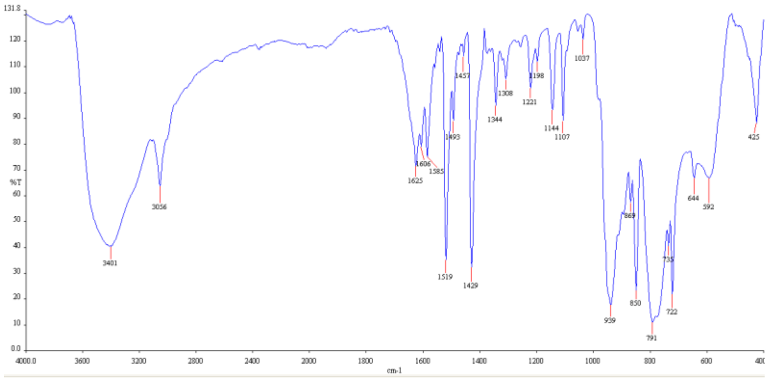

Figure 2. FT-IR spectrum of **1**

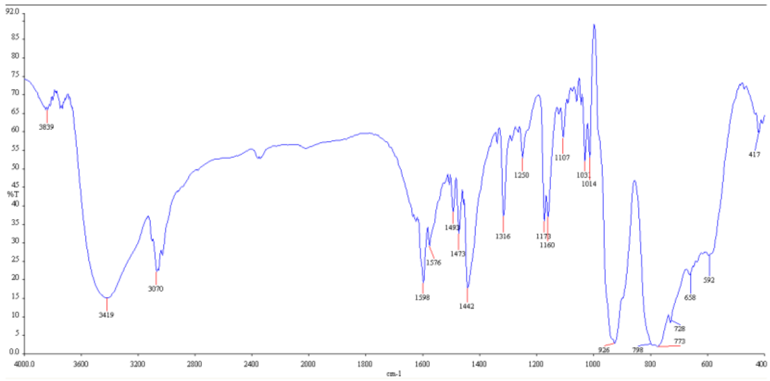

Figure 3. FT-IR spectrum of **2**

The ^{1}H NMR data of compounds **1** and **2** in dimethyl sulfoxide (DMSO-d_6) are as follows: singlet peaks of compound **1** were revealed at 7.82 ppm (18H, CH), 8.02 (18H, CH), 8.51 (18H, CH), 9.13 (18H, CH) and **2** revealed the singlet CH protons δ 7.49 (14H), 7.99 (14H), 8.44 (14H), 8.73 (14H). The ^{1}H NMR data support the proposed structure for both **1** and **2** (Figure 4-5).

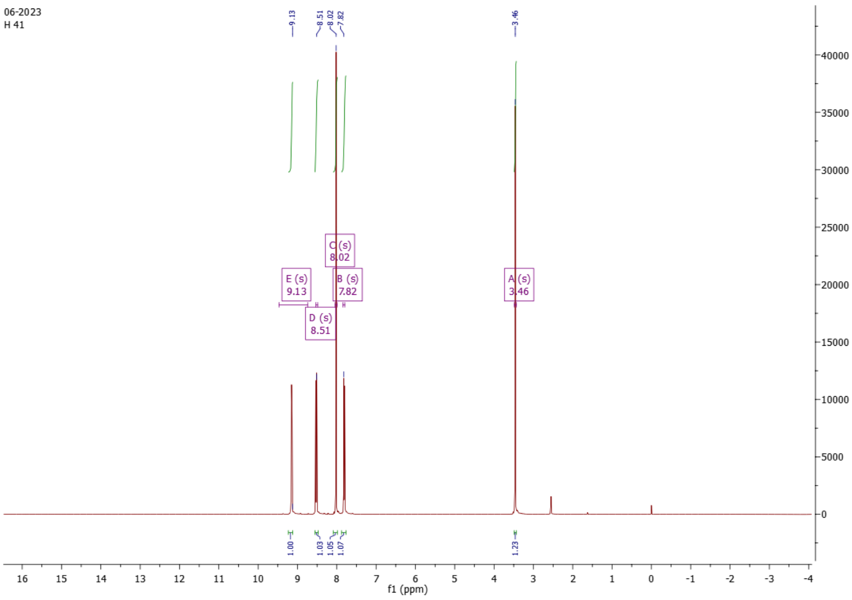

Figure 4. ^{1}H NMR spectrum of **1**

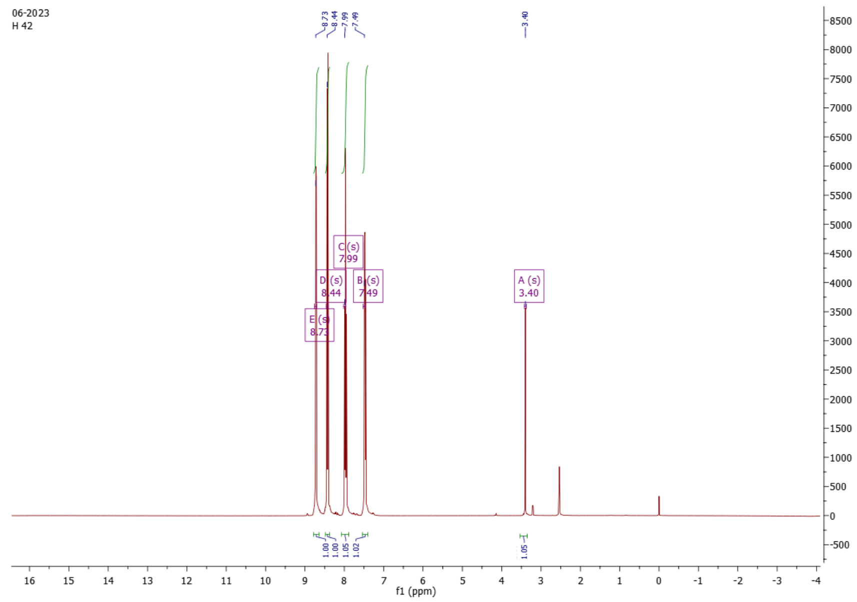

Figure 5. ^{1}H NMR spectrum of **2**

TGA data from **1** (Figure 6) shows that 3.1% weight loss between 30-68 ^{o}C can be assigned to approximately four water molecules in the crystal lattice, while between 70-130 °C, 7.6% can be assigned to removal of three Cu. The 43.43% weight loss between 131-781 ^{o}C is assigned to the removal of six 1,10-phen molecules. The TGA curves of **2** (Figure 6) exhibits the three weight-loss steps between 25 °C and 800 °C too. The 3.58% weight loss of **2** is due to the loss of lattice water in the temperature range of 31°C-64°C. The 8.66% weight loss between 65-194 ^{o}C can be assigned to three Cu. The 41.21% weight loss between 195-781 ^{o}C is assigned to the removal of six 1,10-phen molecules. The cluster is stable up to 800 ^{o}C.

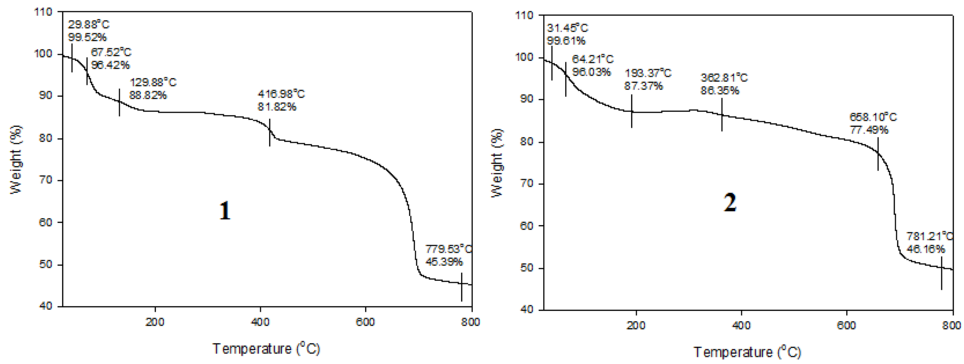

Figure 6. TGA curves of **1** and **2**

Antibacterial Properties

The antibacterial activity of **1** and **2** were studied against *S. aureus* ATCC 25923 (gram positive bacteria) and *E. coli* ATCC 25922 (gram negative bacteria). Table 1 and Figure 7-8 show the results of the antibacterial activities. Compounds **1** and **2** exhibit inhibitory activity against both microorganisms. Compounds **1** and **2** demonstrated strong antibacterial activity against *S. aureus* and *E. Coli*, with inhibition zones of 35 mm and 23 mm, respectively, comparable to the standard drugs Erythromycin. Although these compounds showed antibacterial activity compared to Erythromycin standard, further modification of their structures may help to increase their bioactivities. The results obtained are in agreement with those reported on POM derivatives and their antimicrobial activities. In addition, studies in the literature show that compounds containing 1,10-phenanthroline/2,2'-bipyridine groups have high antimicrobial activity against both gram positive and gram negative bacteria (Abebe et al., 2020; Olar et al., 2021; Tirsoaga et al., 2023).

Table 1. Antibacterial activity of **1,2**, antibiotic, and control group

Microorganisms (Inhibition zone, mm)	**Compounds [a]**		**Antibiotic**	**Control**
	1	**2**	**Erythromycin**	**DMSO**
S. aureus	34	30.5	35	CZ
E. coli	19.5	14	23	CZ

[a] Diameter of the inhibition zone in millimetres, CZ: Contact zone.

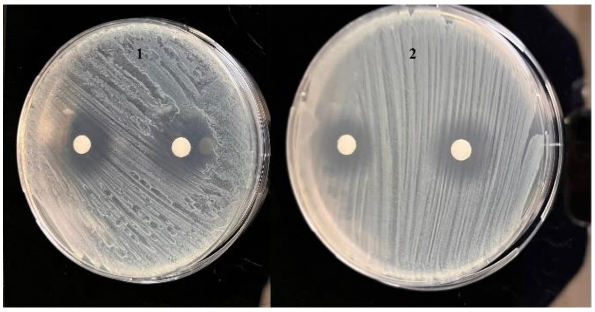

Figure 7. Antibacterial activity of **1** and **2** aganist *E. coli* ATCC 25922

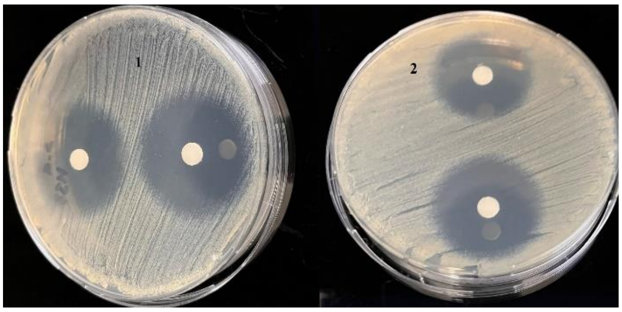

Figure 8. Antibacterial activity of **1** and **2** aganist *S. aureus* ATCC 25923

CONCLUSION

To conclude, $[Cu(phen)_2]_3[Mo_6V_2O_{26}]\cdot 4H_2O$ **(1)** and $[Cu(bpy)_2]_3[Mo_6V_2O_{26}]\cdot 4H_2O$ **(2)** were synthesized and characterized. **1** and **2** were studied as antibacterials against *S. aureus* and *E. coli* respectively. This is the first study in which POM compounds containing $[Mo_6V_2O_{26}]^{6-}$ anion showed antibacterial properties.

REFERENCES

Abebe, A., Bayeh, Y., Belay, M., Gebretsadik, T., Thomas, M., Linert, W. (2020). Mono and binuclear cobalt(II) mixed ligand complexes containing 1,10-phenanthroline and adenine using 1,3-diaminopropane as a spacer: synthesis, characterization, and antibacterial activity investigations. *Future Journal of Pharmaceutical Sciences*, 6, 13.

Avcı Özbek, H., Kopar, E., Demirhan, F. (2021). Synthesis, structure, and antimicrobial properties of mixed-metal organometallic polyoxometalates. $[Cp^*{}_2M_5VO_{17}]^-$ (M=Mo, W). *Journal of Coordination Chemistry*, 74, 1794-1809.

Avcı Özbek, H. (2023). V-subtituted lindqvist-type polyoxometalates: preparation, structural characterization and antibacterial activity. *Chemical Papers,* 77, 5663-5669.

Bijelic, A., Aureliano, M. and Rompel, A. (2015). The antibacterial activity of polyoxometalates: structures, antibiotic effects and future perspectives. *Chemical Communications*, 54, 1153-1169.

Bijelic, A., Rompel, A. (2015). The use of polyoxometalates in protein crystallography – An attempt to widen a well-known bottleneck. *Coordination Chemistry Reviews.* 299, 22-38.

Bildirici, I., Cetin, A., Menges, N., Alan Y. (2023). Synthesis and SAR studies of pyrazole-3-carboxamides and -3-carbonyl thioureides including chiral moiety: Novel candidates as antibacterial agents. *Journal of the Serbian Chemical Society. 83* (7-8), 795-807.

Björnberg, A., (1975). Multicomponent polyanions. 26. The crystal structure of $Na_6Mo_6V_2O_{26}(H_2O)_{16}$, a compound containing sodium-coordinated hexamolybdodi vanadate anions. *Acta Crystallographica*, B35, 1995-1999.

Buvailo, H.I., Makhankova, V.G., Kokozay, V.N., Omelchenko, I. V., Shishkina,S. V., Jezierska, J., Pavliuk M.V., Shylin, S.I. (2019). Copper-containing hybrid compounds based on extremely rare $[V_2Mo_6O_{26}]^{6-}$ POM as water oxidation catalysts. *Inorganic Chemistry Frontiers*, 6, 1813–1823.

Cetin, A., & Korkmaz, A. (2018). Synthesis, optical and morphological properties of novel pyrazole-based oligoamide film. *Optical Materials*, *85*, 79-85.

Cetin, A., Korkmaz, A., Erdoğan, E., & Kösemen, A. (2019). A study on synthesis, optical properties and surface morphological of novel conjugated oligo-pyrazole films. *Materials Chemistry and Physics*, *222*, 37-44.

Cindrić, M., Strukan, N., Vrdoljak, V., Devčić, M., Kamenar, B. (2002). Synthesis of Molybdovanadates Coordinated by Oxalato Ligands. The Crystal Structure of $K_6[Mo_6V_2O_{24}(C_2O_4)_2]\cdot 6H_2O$. *Journal of Coordination Chemistry*, 55 (6), 705-710.

Fei, F., An, H., Meng, C., Wang, L., Wang, H. (2015). Lanthanide-supported molybdenum–vanadium oxide clusters: syntheses, structures and catalytic properties. *RSC Advances*, 5, 18796–18805.

Han, P.P., Li, J., Xing, C.L., Zhao, M., Han, Q.X., Li, M.X., 2019. Octamolybdate-based hybrids for direct conversion of aldehydes and ketones to oximes. *Inorganic Chemistry Communications*, 110, 107592.

Hegde, A., Kabra S., Basawa, R.M., Khile, D. A., Abbu, R.U.F., Thomas, N.A., Manickam, N.B., Raval1, R. (2023). Bacterial diseases in marine fish species: current trends and future prospects in disease management. *World Journal of Microbiology and Biotechnology*. 39, 317.

Gao, Q., Qi, B., Wu, T., Xu, L. (2019). A novel organic-inorganic hybrid built upon molybdovanadate cluster of $[V_2Mo_6O_{26}]^{6-}$ and {Gd(DMF)3(H2O)} units with electrochemical sensing of nitrite. *Inorganic Chemistry Communications.* 107, 107481.

Gong, Z., Guo, C., Wang, J., Chen, S., Hu, G. (2023). Establishment and identification of a skin cell line from Chinese tongue sole (*Cynoglossus semilaevis*) and analysis of the changes in its transcriptome upon LPS stimulation. *Fish and Shellfish Immunology*. 142, 109119.

Korkmaz, A. Cetin, A., Kaya, E., Erdoğan, E. (2018). Novel polySchiff base containing naphthyl: synthesis, characterization, optical properties and surface morphology. *Journal of Polymer Research*. 25, 178.

Lentink, S., Marcano, D. E. S., Moussawi, M. A., Parac-Vogt, T. N. (2023). Exploiting Interactions between Polyoxometalates and Proteins for Applications in (Bio)chemistry and Medicine. *Angewandte Chemie-International Edition*. e202303817.

Luo, Z., Kögerler, P., Cao, R., Hakim, I., Hill, C.L. (2008). Synthesis, structure and magnetism of a new dimeric silicotungstate: $K_9N_2Cu_{0.5}[\gamma\text{-}Cu_2(H_2O)SiW_8O_{31}]_2\cdot 38H_2O$. *Dalton Transactions.* 143 (1), 54-58.

Manikandan, D.B., Arumugam, M., Abdul, U., Sridhar, A., Kari, Z.A., Téllez-Isaías, G., Ramasamy, T. (2023). Green synthesized AgNPs, CuONPs, and Ag-CuO NCs to effective antibiofilm activities and their potential application in aquaculture. *Applied Organometallic Chemistry*. e7293.

Mousavi, S.M., Hashemi, S.A., Mazraedoost, S., Chiang, W.H., Yousefi, K., Arjmand, O., Ghahramani, Y., Gholami, A., Omidifar, N., Rumjit, N.P., Salari, M., Sadrmousavi-Dizaj, A. (2022). Anticancer, antimicrobial and biomedical features of polyoxometalate as advanced materials: A review study. *Inorganic Chemistry Communications.* 146, 110074.

Nenner, A.N. (1985). Multicomponent Polyanions. 38. Structure of $K_5NaMo_6V_2O_{26}.4H_2O$, a Compound Containing a New Configuration of the Hexamolybdodivanadate Anion. *Acta Crystallographica*, C41, 1703-1707.

Olar, R., Badea, M., Bacalum, M., Raileanu, M., Rutaˇ, L.L., Farcasanu, I.C., Rostas, A.M., Vlaicu, I.D., Popa, M., Chifiriuc, M.C. (2021). Antiproliferative and antibacterial properties of biocompatible copper(II) complexes bearing chelating N,N-heterocycle ligands and potential mechanisms of action. *Biometals*. 34, 1155-1172.

Song, F., Wang, T. (2022). Application of Polyoxometalates in Chemiresistive Gas Sensors: A Review. *ACS Sensors*, 7, 12, 3634–3643.

Tirsoaga, A., Cojocaru, V., Badea, M., Badea, I.A., Rostas, A.M., Stoica, R., Bacalum, M., Chifiriuc, M.C., Olar, R. (2023). Copper (II) Species with Improved Anti-Melanoma and Antibacterial Activity by Inclusion in β-Cyclodextrin. *International Journal of Molecular Sciences*. 24, 2688.

Wang, J., Wang, J., MA, P., Niu J. (2009). Hydrothermal synthesis and crystal structure of a 1-D compound constructed from molybdovanadate clusters $[V_2Mo_6O_{26}]^{6-}$ and copper complexes. *Journal of Coordination Chemistry*, 62 (16), 2641-2647.

Wang, S., Sun, W., Hu, Q., Yan, H., Zeng, Y. (2017). Synthesis and evaluation of pyridinium polyoxometalates as anti-HIV-1 agents. *Bioorganic & Medicinal Chemistry Letters*, 27(11), 2357–2359.

Xing, C., Ma, M., Chang, J., Ji, Z., Wang, P., Sun, L., Li, S., Li, M. (2023). Polyoxometalate anchored zinc oxide nanocomposite as a highly effective photocatalyst and bactericide for wastewater decontamination. *Chemical Engineering Journal*, 464, 142632.

Yang, Y., Ma, S., Li, T., He, J., Liu, S., Liu, H., Zhang, J., Zhou, X., Liu, L., Yang, S. (2023). Discovery of novel ursolic acid derivatives as effective antimicrobial agents through a ROS-mediated apoptosis mechanism. *Frontiers of Chemical Science and Engineering*.

Zhao, M., Fang, Y., Ma, L., Zhu, X., Jiang, L., Li, M., Han, Q. (2020). Synthesis, characterization and in vitro antibacterial mechanism study of two Keggin-type polyoxometalates. *Journal of Inorganic Biochemistry*, 210, 111131.